THE JOURNAL OF PHYSICAL CHEMISTRY B

Article

pubs.acs.org/JPCB

Theoretical Study of the Binding Energy of a Methane Molecule in a $(H_2O)_{20}$ Dodecahedral Cage

Michael J. Deible, Odbadrakh Tuguldur, and Kenneth D. Jordan*

Department of Chemistry, University of Pittsburgh, Pittsburgh, Pennsylvania 15260, United States

Supporting Information

ABSTRACT: The interaction energy of a methane molecule encapsulated in a dodecahedral water cage is calculated using the MP2, MP2C, various dispersion-corrected DFT, and diffusion Monte Carlo (DMC) methods. The MP2, MP2C, and DMC methods give binding energies of −5.04, −4.60, and −5.3 ± 0.5 kcal/mol, respectively. In addition, the two- and three-body contributions are evaluated using the DFT, MP2, and CCSD(T) methods. All of the DFT methods considered appreciably overestimate the magnitude of the three-body contribution to the interaction energy. The two- and three-body energies are further analyzed by use of symmetry-adapted perturbation theory (SAPT) which allows decomposition into electrostatics, exchange, induction, and dispersion contributions. The SAPT calculations reveal that the induction, dispersion, and exchange three-body contributions to the methane-cage binding energy are all sizable, with the net three-body contribution to the binding energy being about 1 kcal/mol.

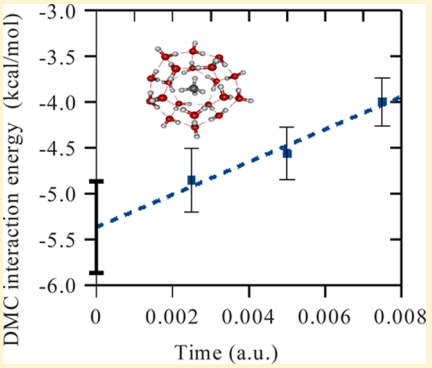

INTRODUCTION

It is estimated that there are about 10^{16} kg of methane trapped in methane hydrate clathrate deposits on the ocean floor and in the permafrost.[1] As a result, methane hydrate has attracted considerable attention as a possible source of natural gas and because of the environmental consequences of its decomposition; the later concern derives from the fact that CH_4 is a potent greenhouse gas.

The most common form of methane hydrate has a type I hydrate structure, with the unit cell consisting of two 5^{12} and six $5^{12}6^2$ water cages,[2,3] with a methane molecule in the center of each cage. The 5^{12} cage has a dodecahedral structure, while the 24-molecule $5^{12}6^2$ cage has 12 pentagonal faces and 2 opposing hexagonal faces. Numerous computational studies have been carried out on the properties of methane hydrate crystal (for example, see ref 4 and references therein) as well as on the $CH_4@(H_2O)_{20}$ gas-phase cluster with a methane encapsulated in an $(H_2O)_{20}$ dodecaheral cage.[5−8] The isolated $CH_4@(H_2O)_{20}$ system has been studied using a wide range of electronic-structure methods, with various dispersion-corrected density functional theory (DFT) methods giving binding energies between −4 and −7 kcal/mol.[5−8] The complete-basis-set (CBS) limit MP2 binding energy has been estimated to be −6.1 kcal/mol.[5] However, the extrapolation to the CBS limit in ref 5 was done using energies obtained with only the aug-cc-pVDZ and aug-cc-pVTZ basis sets,[9] a strategy which is known to be inadequate.[10] In the force field studies of crystalline methane hydrate, it has generally been assumed that three- and higher-body interactions are not important for describing the interaction of the methane molecule with the water cage, although, in a paper from our group, it was reported that inclusion of polarization effects significantly impacts the thermal conductivity.[11]

The lack of agreement of the various theoretical results for the stability of a methane molecule in the $(H_2O)_{20}$ cage and the paucity of information on the role of three-body interactions on the binding of the methane in the water cage has motivated us to undertake diffusion Monte Carlo and near CBS-limit MP2 and MP2C[12,13] calculations of the binding energy as well as to calculate the two- and three-body contributions to the methane−$(H_2O)_{20}$ binding energy at various levels of theory, including CCSD(T)-F12,[14,15] DF-MP2-F12,[13] DF-MP2C-F12,[12,13] and symmetry-adapted perturbation theory (SAPT).[16−18]

COMPUTATIONAL DETAILS

The dodecahedral water cage has 30 026 symmetry distinct isomers with different arrangements of the protons.[19] In the present study, we employ the lowest energy isomer identified by Kirov et al.[20] which corresponds to structure 15 in a study by Wales and Hodges.[21] The geometries of the empty water cage and of the isolated methane molecule were optimized using second-order Møller−Plesset theory[22] with density fitting (DF-MP2)[23] together with the aug-cc-pVDZ basis set. The methane molecule was then placed in the water cage with the carbon located at the cage's center, and the orientation of the methane was optimized at the M06-2X[24]/aug-cc-pVDZ level of theory, keeping all other degrees of freedom frozen. The

Special Issue: James L. Skinner Festschrift

Received: February 13, 2014
Revised: April 12, 2014

   dx.doi.org/10.1021/jp501592h | J. Phys. Chem. B XXXX, XXX, XXX−XXX

resulting geometry parameters are similar to those of earlier *ab initio* studies of $CH_4@(H_2O)_{20}$,[5] and are reported in the Supporting Information. These geometries were used for all subsequent calculations. The optimized structure of $CH_4@(H_2O)_{20}$ is shown in Figure 1.

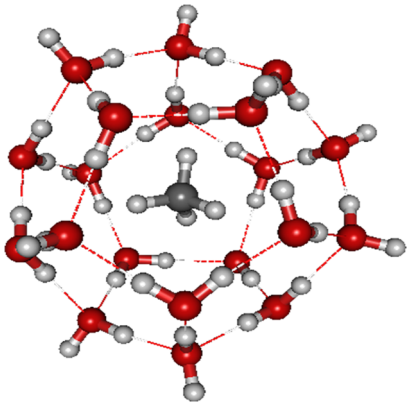

Figure 1. Geometry of the methane hydrate structure studied. Red atoms are oxygen, white are hydrogen, and gray is carbon.

Net interaction energies were calculated using

$$E_{int} = E_{CH_4@(H_2O)_{20}} - E_{(H_2O)_{20}} - E_{CH_4} \quad (1)$$

The DFT calculations made use of the BLYP,[25] M06-2X,[24] PBE,[26] and PBE0[27] functionals together with the aug-cc-pVTZ basis set and density fitting. The PBE0 functional is a hybrid functional with 25% exact exchange, and M06-2X is a hybrid meta functional with 54% exact exchange. The BLYP, PBE, and PBE0 calculations were carried out with and without the D3 dispersion correction of Grimme et al.[28] In addition, supermolecule calculations were carried out using the DF-MP2 and DF-MP2C-F12[12,13] methods, where DF refers to the use of density fitting[29,30] and F12[13−15] refers to an explicitly correlated method that gives energies that would otherwise require much larger Gaussian basis sets. The dispersion energy at the MP2 level can be shown to be equivalent to the use of uncoupled Hartree−Fock (HF) monomer polarizabilities in the Casimir−Polder expression.[12] The MP2C method replaces the uncoupled HF polarizabilites in the MP2 contribution to the dispersion energy with coupled Kohn−Sham polarizabilities and, thus, can yield accurate interaction energies for systems for which the MP2 method fares poorly.[12] The DF-MP2C-F12 calculations were carried out using the aug-cc-pVTZ basis set.[9] For the DF-MP2 calculations, complete basis-set-limit results were obtained by extrapolating the energies from calculations using the aug-cc-pVDZ, aug-cc-pVTZ, and aug-cc-pVQZ basis sets.[9] The methods of Feller[31] and Helgaker et al.[32] were used for extrapolation of the Hartree−Fock and correlation contributions, respectively. The interaction energies calculated using the various DFT and wave function methods listed above were corrected for basis set superposition error (BSSE) using the counterpoise method.[33] These calculations were carried out using the MOLPRO[34] code.

The diffusion Monte Carlo (DMC) method was also used to obtain an accurate value of the net binding energy. For the trial wave functions, Slater determinants of B3LYP[35] orbitals were generated using Trail−Needs pseudopotentials[36] on all atoms and the valence triple-ζ basis sets of Xu et al.[37] without the f functions or supplemental diffuse functions. These basis sets were designed for use with the Trail−Needs pseudopotentials. The Slater determinants were combined with Jastrow factors[38] with electron−electron, electron−nucleus, and electron−electron−nucleus terms, optimized via the variational Monte Carlo (VMC) procedure with variance minimization. The trial functions impose the fixed-node approximation, which should cause a negligible error in the binding energy. The T-move[39] scheme was used to account for the nonlocality of the pseudopotentials. Time step bias was removed by use of three time steps of 0.0025, 0.005, and 0.0075 au for extrapolation to zero time step. The B3LYP calculations for the generation of the trial function were carried out with Gaussian 09,[40] and the DMC calculations were carried out with the CASINO[41] code.

The two- and three-body energies were calculated using

$$\Delta E_2^j = [E(m, j) - E(m) - E(j)] \quad (2)$$

and

$$\Delta E_3^{(j,k)} = E(m, j, k) - E(m, j) - E(m, k) - E(j, k) + E(m) + E(j) + E(k) \quad (3)$$

where m refers to the methane molecule and j and k refer to water monomers. Because each monomer was held to a rigid geometry, there is no one-body contribution. The two- and three-body contributions to the binding energy were calculated at the CCSD(T)-F12b[14] and DF-MP2-F12[13] levels with the VTZ-F12[42] basis set as well as with each of the density functional methods considered using the aug-cc-pVTZ basis set. The two- and three-body energies were corrected for BSSE using the counterpoise method. The two-body contribution was also calculated using the DF-MP2C-F12 method together with the VTZ-F12 basis set.

The two- and three-body energies were dissected into physical contributions by use of the DF-DFT-SAPT[16] and HF-based SAPT[17,18] methods, respectively. The DF-DFT-SAPT and HF-based SAPT calculations were carried out using the aug-cc-pVTZ basis set and aug-cc-pVDZ basis set, respectively, and, by design, are free of BSSE. The two-body SAPT calculations dissect the net two-body energy into electrostatics, exchange, induction, exchange−induction, dispersion, and exchange−dispersion contributions. There is also a so-called δHF contribution which we combine with induction and exchange induction to obtain an estimate of the net induction. For the two-body DF-DFT-SAPT calculations, the PBE0 functional[27] was used with an asymptotic correction for the ionization potential. The adiabatic local density approximation (ALDA)[43] kernel was used in the calculation of the response functions employed to evaluate the dispersion contribution. The three-body SAPT energies include exchange, induction, exchange−induction, dispersion, and exchange−dispersion contributions. There are both second- and third-order contributions to the three-body induction contribution, and again, there is a δHF correction which we incorporate in the net induction.

In calculating the net two-body SAPT contributions, two different strategies were pursued, one following the usual approach which involves summing the contributions for each methane−water dimer in the $CH_4@(H_2O)_{20}$ complex and the second treating the $(H_2O)_{20}$ cluster as a single molecule. For the first strategy, experimental IPs for methane and H_2O were used for the asymptotic correction. For the second strategy, the experimental IP of methane was again used, but the Hartree−Fock Koopmans' theorem[44] estimate of the IP was used in the

dx.doi.org/10.1021/jp501592h | J. Phys. Chem. B XXXX, XXX, XXX−XXX

asymptotic correction for the $(H_2O)_{20}$ cluster. The three-body SAPT energy was calculated by considering all methane−$(H_2O)_2$ trimers extracted from the $CH_4@(H_2O)_{20}$ system.

RESULTS AND DISCUSSION

1. Supermolecule Interaction Energies. Table 1 summarizes the net methane−$(H_2O)_{20}$ binding energies obtained at the various levels of theory. The DMC calculations give a binding energy of −5.3 ± 0.5 kcal/mol, which, to within statistical uncertainty, agrees with our CBS MP2 binding energy of −5.04 kcal/mol. (The data used in the extrapolation of the DMC results to zero time step are shown in Figure 2.) We note that our methane binding energy for the $CH_4@(H_2O)_{20}$ cluster system is also in excellent agreement with a recent DMC result of −5.6 ± 0.3 kcal/mol for crystalline methane hydrate.[45] Our best estimate of binding energy, derived from the *N*-body decomposition discussed below, is −5.2 kcal/mol. The close agreement of the MP2 result with the DMC and best estimate values is, in part, fortuitous, as the MP2 method has errors of about +0.8 and −0.9 kcal/mol in the two- and three-body interactions, respectively. The MP2C-F12 method with the aug-cc-pVTZ basis set gives a net binding energy of −4.6 kcal/mol, but this result may be slightly underestimated in magnitude due to the basis set employed.

Table 1. Energy (kcal/mol) for Binding of a Methane Molecule in a $(H_2O)_{20}$ Cage with the Structure Given in Figure 1

method[a]	interaction energy
DF-HF[b]	4.13
PBE	1.31
PBE-D3	−6.61
PBE0	1.07
PBE0-D3	−6.89
BLYP	5.92
BLYP-D3	−6.72
M06-2X	−5.70
DF-MP2[b]	−5.04
DF-MP2C-F12	−4.60
DMC[c]	−5.3(5)

[a]The DFT and DF-MP2C-F12 calculations used the aug-cc-pVTZ basis set, and the binding energies include the counterpoise correction for BSSE. [b]Extrapolated to the complete-basis-set limit as described in the text. [c]The DMC calculations were carried out as described in the text.

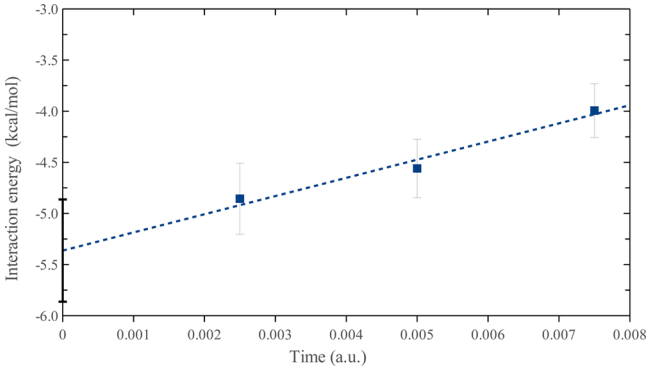

Figure 2. Time step extrapolation of the DMC interaction energy. Interaction energy is solved as in eq 1 at each time step (solid blocks, with error bars), and a linear fit is used to extrapolate to zero time step (dashed line).

2. Two-Body Interaction Energies. Table 2 lists, for the various theoretical methods considered, the two-body contributions to the methane−$(H_2O)_{20}$ interaction energy. The CCSD(T)-F12b value for the two-body interaction energy, which is expected to be the most accurate result, is −5.85 kcal/mol. In comparison, the DF-MP2-F12 and DF-MP2C-F12 methods give two-body interaction energies of −4.95 and −5.54 kcal/mol, respectively. Thus, it is seen that the MP2 method significantly (by 0.9 kcal/mol) underestimates the magnitude of the two-body interaction energy, while the MP2C method fares much better.

Table 2. Two-Body Interaction Energies (kcal/mol)

method[a]	interaction energy
DF-HF	3.85
PBE	−3.88
PBE-D3	−11.81
PBE0	−2.36
PBE0-D3	−10.28
BLYP	6.31
BLYP-D3	−6.34
M06-2X	−5.22
DF-MP2-F12	−4.95
DF-MP2c-F12	−5.54
CCSD(T)-F12b	−5.85

[a]The HF and DFT calculations were carried out using the aug-cc-pVTZ basis set, while the DF-MP2C-F12, DF-MP2-F12, and CCSD(T)-F12b calculations were carried out using the VTZ-f12 basis set. All results are corrected for BSSE with the counterpoise method.

The only DFT methods that give two-body contributions within 0.6 kcal/mol of the CCSD(T)-F12b result are BLYP-D3 and M06-2X which give two-body contributions of −6.34 and −5.22 kcal/mol, respectively. Both the PBE and PBE0 functionals give a bound $CH_4@(H_2O)_{20}$ complex at the two-body level, albeit underestimating the binding. In contrast, at the HF level of theory, the two-body contribution is repulsive

dx.doi.org/10.1021/jp501592h | J. Phys. Chem. B XXXX, XXX, XXX−XXX

by 3.85 kcal/mol. While some of the binding with the PBE and PBE0 functionals at the two-body level could be due to their recovering short-range (i.e., overlap dependent) intermonomer correlation effects, much of the binding found with these two functionals is due to their underestimating exchange−repulsion.[47] Not surprisingly, the PBE-D3 and PBE0-D3 methods give far too attractive two-body contributions to the binding energy.

The DFT-SAPT analysis of the two-body contributions to the binding energy is reported in Table 3, from which it is seen

Table 3. DF-DFT-SAPT Energy (kcal/mol) Decomposition of the Two-Body Interaction Energy of $CH_4@(H_2O)_{20}$

contribution[a]	treating each H_2O−methane pair separately	treating the $(H_2O)_{20}$ as a single molecule
$E_{es}^{(1)}$	−3.15	−3.08
$E_{exch}^{(1)}$	10.04	9.74
$E_{ind}^{(2)}$	−3.15	−2.29
$E_{exch-ind}^{(2)}$	1.97	2.24
$E_{\delta HF}$	−0.38	−0.30
E_{ind}^{net}	−1.57	−0.36
$E_{disp}^{(2)}$	−12.64	−11.60
$E_{exch-disp}^{(2)}$	1.25	1.40
E_{disp}^{net}	−11.39	−10.19
E_{SAPT}	−5.88	−3.88

[a]The DF-DFT-SAPT calculations were carried out using the aug-cc-pVTZ basis set.

that the electrostatics, exchange−repulsion, induction, and exchange−induction contributions to the two-body energy are −3.15, 10.04, −3.15, and 1.97 kcal/mol, respectively. There is also a small δHF contribution of −0.38 kcal/mol. The net induction contribution, defined as $E_{ind}^{net} = E_{ind} + E_{ind}^{ex} + E_{\delta HF}$, to the two-body interaction energy is −1.57 kcal/mol. Thus, two-body induction is surprisingly important in the interaction of the methane molecule with the $(H_2O)_{20}$ cage.

The sum of the DFT-SAPT interactions considered thus far is 5.71 kcal/mol, which is 1.86 kcal/mol more repulsive than the HF value of the two-body interaction energy. Thus, electron correlation effects significantly destabilize the electrostatics + exchange−repulsion + induction contribution to the two-body binding energy of $CH_4@(H_2O)_{20}$. The DFT-SAPT calculations give two-body dispersion and exchange−dispersion contributions of −12.64 and 1.25 kcal/mol, respectively. Adding these two contributions to the nondispersion contributions discussed above gives a net two-body contribution energy of −5.88 kcal/mol, nearly identical to the CCSD(T)-F12b result.

We also carried out DFT-SAPT calculations treating the entire $(H_2O)_{20}$ cage as a single molecule. The DFT-SAPT calculations treating the $(H_2O)_{20}$ as a single molecule give essentially the same electrostatics energy, and a value of the exchange−repulsion energies only 0.3 kcal/mol smaller than that obtained by treating the water molecules individually. On the other hand, the net induction and dispersion contributions are each about 1.2 kcal/mol less stabilizing in the former approach. The different induction and dispersion contributions obtained from the two types of "two-body" DFT-SAPT analysis can be understood in terms of the fact that treating $(H_2O)_{20}$ as a single molecule incorporates some contributions that would be considered many-body in a procedure where one builds up the cluster one molecule at a time. We return to the issue of the similar exchange−repulsion interactions obtained using the two SAPT approaches described above after considering the three-body interaction energies.

3. Three-Body Interaction Energies. The three-body interaction energies are summarized in Table 4. The net three-body interaction energy is calculated to be −0.28, 0.25, and 1.01 kcal/mol at the HF, DF-MP2-F12, and CCSD(T)-F12b levels of theory, respectively. The CCSD(T)-F12b value of the net three-body energy is 0.76 kcal/mol more repulsive than the corresponding MP2-F12 value, consistent with the importance of the Axilrod−Teller three-body dispersion contribution which appears at third-order perturbation theory. The various DFT methods give values of the three-body interaction energies ranging from −2.79 to 7.53 kcal/mol, with only the M06-2X functional giving a three-body interaction energy within 1 kcal/mol of the CCSD(T) result.

Table 4. Three-Body Contributions to the Binding Energy (kcal/mol) of a Methane Molecule in the $(H_2O)_{20}$ Cage

method[a]	30 H-bonded dimer pairs	160 dimer pairs without H-bonds	total 3-body interaction energy
HF	−1.48	1.20	−0.28
PBE	3.17	4.36	7.53
PBE0	1.50	2.95	4.45
BLYP	−2.37	−0.41	−2.79
M06-2X	−1.23	2.87	1.64
DF-MP2-F12	−0.96	1.21	0.251
CCSD(T)-F12b	−0.42	1.43	1.01
HF-SAPT Energy Decomposition			
$E_{exch}^{(1)}$	−1.31	−0.01	−1.32
$E_{ind}^{(2)}$	−0.05	0.85	0.80
$E_{ind}^{(3)}$	−0.41	0.01	−0.40
$E_{exch-ind}^{(2)}$	−0.02	0.06	0.04
$E_{\delta HF}$	0.29	0.33	0.62
E_{ind}^{net}	−0.19	1.25	1.06
$E_{disp}^{(3)}$	0.41	0.22	0.63
$E_{exch-disp}^{(2)}$	0.71	0.13	0.84
E_{disp}^{net}	1.12	0.35	1.47
HF-SAPT	−0.37	1.57	1.21

[a]The HF-SAPT calculations were carried out using the aug-cc-pVDZ basis set. The DF-MP2-F12 and CCSD(T)-F12b calculations were carried out using the VTZ-f12 basis set, and the DFT calculations were carried out using the aug-cc-pVTZ basis set. These results include the counterpoise correction for BSSE.

Table 4 also summarizes the results of the three-body SAPT calculations on the $CH_4@(H_2O)_{20}$ system. The exchange, induction, and exchange−induction three-body contributions are −1.3, 0.4, and 0.0 kcal/mol, respectively, while the δHF contribution is 0.6 kcal/mol. Combining the induction, exchange−induction, and δHF contributions, we obtain a net three-body induction contribution of 1.1 kcal/mol for the binding of the methane molecule in the $(H_2O)_{20}$ cage. Recalling that the net two-body induction contribution was about −1.6 kcal/mol, we see that the combined two- plus three-body induction contribution is only −0.5 kcal/mol. The three-body dispersion and exchange−dispersion contributions are 0.6 and 0.8 kcal/mol, respectively. The overall three-body contribution to the methane binding obtained using the SAPT method is 1.3 kcal/mol in reasonable agreement with the CCSD(T) result of 0.9 kcal/mol. If we simply add the SAPT three-body dispersion and exchange−dispersion contribution to the DFT three-body energies, the PBE and PBE0

dx.doi.org/10.1021/jp501592h | J. Phys. Chem. B XXXX, XXX, XXX−XXX

results would be even further removed from the CCSD(T)-F12b result, while the BLYP result for the three-body interaction energy would still differ from the CCSD(T)-F12b result by 2.4 kcal/mol. It is clear that some deficiency other than the neglect of long-range dispersion interactions is responsible for the large errors in the PBE, PBE0, and BLYP three-body contributions to the binding of CH_4 in the $(H_2O)_{20}$.

It is instructive to further decompose the three-body contributions into two parts, that due to the 30 trimers with the two water monomers H-bonded to one another, referred to as set A, and that due to the 160 trimers without H-bonding between the two water monomers, referred to as set B. From Table 3, it is seen that while the CCSD(T) three-body energy is −0.4 kcal/mol for set A trimers, it is 1.5 kcal/mol for set B. The corresponding MP2-F12 results are −1.0 and 1.2 kcal/mol. None of the DFT methods considered closely reproduces the CCSD(T) values of the three-body interaction energy of either the A- or B-type trimers. Table 4 also reports the three-body SAPT contributions for the two types of trimers. From the table, we see that the three-body exchange contribution derives almost entirely from the set A trimers, while the three-body induction (including the δHF term) is dominated by the set B trimers. The three-body dispersion is dominated by the A-type trimers.

It was noted in the previous section that the differences in the SAPT values of the two-body induction, exchange, and dispersion contributions to the methane binding energy as calculated treating each monomer separately and treating the $(H_2O)_{20}$ cage as a single molecule are 1.24, −0.30, and 1.18 kcal/mol, respectively. From Table 4, it is seen that for induction and dispersion these differences are comparable to the corresponding three-body contributions (calculated using all methane−$(H_2O)_2$ trimers). This is consistent with the fact that the DFT-SAPT "two-body" calculations treating the entire $(H_2O)_{20}$ as a single monomer include a subset of the $N \geq$ three-body interactions as evaluated treating the water monomers as separate molecules. On the other hand, the three-body exchange−repulsion contribution of −1.32 kcal/mol is about 1.0 kcal/mol larger in magnitude than the difference of the two-body exchange contributions calculated using the two strategies described above. Examination of the various contributions to the three-body exchange energy reveals that about half of this discrepancy is due to the three-body exchange contributions that are not recovered in the "two-body" SAPT calculations treating the $(H_2O)_{20}$ as a single monomer.

Table 5 summarizes the two-, three-, and higher-body contributions for the binding of a methane molecule in the $(H_2O)_{20}$ cage. At the HF and DF-MP2 levels of theory, the $N \geq 4$ contributions are only 0.6 and −0.3 kcal/mol, respectively. CCSD(T) calculations for the entire complex with the basis sets used here would be computationally prohibitive. However, if we use the DMC result for the net binding energy, we can obtain an estimate of the CCSD(T)-F12 higher-body contribution to the binding energy. Using this strategy, we obtain a value of −0.5 kcal/mol for the $N \geq 4$ contribution to the binding energy. However, this is subject to a ±0.5 kcal/mol statistical uncertainty due to the use of the DMC value of the net binding energy. In contrast to the small $N \geq 4$-body contribution obtained using the wave function methods, the PBE, M06-2X, and BLYP density functional methods give higher-body contributions of −2.3, −2.1, and 2.4 kcal/mol, respectively. The PBE0 method, on the other hand, gives a higher-body interaction energy of −0.9 kcal/mol, consistent with our expectation that self-interaction is primarily responsible for the large overestimation of the three-body energy by the PBE method. The MP2 and CCSD(T) results presented in Table 5 can be combined to obtain an improved estimate of the net binding energy. In particular, by adding the differences of the CCSD(T) and MP2 values of the two- and three-body interaction energies to the CBS-limit DF-MP2 value of the net binding energy, we obtain a value of −5.2 kcal/mol, which is nearly identical to the DMC result.

Table 5. Energy (kcal/mol) of the *N*-Body Decomposition

		N-body contributions		
method	full	2	3	$N \geq 4$
HF	4.13	3.85	−0.28	0.56
PBE	1.31	−3.88	7.53	−2.34
PBE0	1.07	−2.36	4.45	−1.02
BLYP	5.92	6.31	−2.79	2.40
M06-2X	−5.70	−5.22	1.64	−2.12
DF-MP2-F12	−5.04[a]	−4.95	0.25	−0.34
CCSD(T)-F12b	(−5.3)[b]	−5.85	1.01	(−0.46)[c]

[a]CBS-limit DF-MP2 result. [b]DMC result. [c]Estimated using a DMC value of −5.3 kcal/mol for the full interaction energy.

CONCLUSIONS

The binding energy of a methane molecule in a H_2O_{20} dodecahedral cage was calculated using a variety of electronic structure methods. Diffusion Monte Carlo calculations give a binding energy of −5.3 ± 0.5 kcal/mol, in excellent agreement with our best estimate value of −5.2 kcal/mol, obtained by correcting the CBS-limit MP2 result with the CCSD(T)-F12b − MP2-F12 differences for the two- and three-body contributions to the binding energy. Of the density functional methods tested, only M06-2X gives a binding energy within 1 kcal/mol of our best estimate value. The PBE-D3, PBE0-D3, and BLYP-D3 methods overbind the methane molecule by 1.5−1.8 kcal/mol.

A SAPT analysis reveals that exchange, induction, and dispersion all make important contributions to the three-body interaction energy. Thus, for force field methods to accurately describe the interaction of a methane in an $(H_2O)_{20}$ cage, it will be necessary to include explicit terms for three-body exchange, induction, and dispersion. However, because the net three-body exchange contribution is negative and the three-body induction and dispersion contributions are positive and the three terms are roughly comparable in magnitude, a force field with only induction or dispersion for three-body interactions could fortuitously give a three-body energy close to the *ab initio* result. We also find that none of the density functional methods considered fare well at predicting the two-, three-, and higher-body contributions to the binding energy. It is clear from comparison of the DFT and SAPT results for the two- and three-body contributions to the binding energies that the DFT methods have shortcomings other than those associated with the neglect of long-range dispersion interactions. Strikingly, with the PBE functional, the three-body contribution to the binding energy of the $CH_4@(H_2O)_{20}$ is too large by a factor of 7. To a large extent, this is a result of self-interaction error in the DFT methods. The failure of standard DFT methods to accurately describe the terms in the *N*-body expansion of water clusters and ice has been noted in other recent studies.[48,49] In

dx.doi.org/10.1021/jp501592h | J. Phys. Chem. B XXXX, XXX, XXX−XXX

addition, in a very recent study, Cox and co-workers reported that none of the density functional methods that they examined performed well for the methane hydrate crystal.[45]

■ ASSOCIATED CONTENT

Supporting Information

The coordinates for the methane hydrate cluster as well as geometry parameters. This material is available free of charge via the Internet at http://pubs.acs.org.

■ AUTHOR INFORMATION

Notes

The authors declare no competing financial interest.

■ ACKNOWLEDGMENTS

This research was carried out with the support of NSF grant CHE1111235. An award of computer time was provided by the Innovative and Novel Computational Impact on Theory and Experiment (INCITE) program. This research used resources of the Argonne Leadership Computing Facility at Argonne National Laboratory, which is supported by the Office of Science of the U.S. Department of Energy under contract DE-AC02-06CH11357. We thank Dr. Mike Gillan for valuable discussions.

■ REFERENCES

(1) Buffett, B. A. Clathrate Hydrates. *Annu. Rev. Earth Planet. Sci.* **2000**, *28*, 477−507.
(2) Fleyfel, F.; Devlin, J. P. FT-IR Spectra of 90 K Films of Simple, Mixed, and Double Clathrate Hydrates of Trimethylene Oxide, Methyl Chloride, Carbon Dioxide, Tetrahydrofuran, and Ethylene Oxide Containing Decoupled Water-d2. *J. Phys. Chem.* **1988**, *92*, 631−635.
(3) Fleyfel, F.; Devlin, J. P. Carbon Dioxide Clathrate Hydrate Epitaxial Growth: Spectroscopic Evidence for Formation of the Simple Type-II Carbon Dioxide Hydrate. *J. Phys. Chem.* **1991**, *95*, 3811−3815.
(4) Baghel, V. S.; Kumar, R.; Roy, S. Heat Transfer Calculations for Decomposition of Structure I Methane Hydrates by Molecular Dynamics Simulation. *J. Phys. Chem. C* **2013**, *117*, 12172−12182.
(5) Kumar, P.; Sathyamurthy, N. Theoretical Studies of Host−Guest Interaction in Gas Hydrates. *J. Phys. Chem. A* **2011**, *115*, 14276−14281.
(6) Khan, A. Theoretical Studies of $CH_4(H_2O)_{20}$, $(H_2O)_{21}$, $(H_2O)_{20}$, and Fused Dodecahedral and Tetrakaidecahedral Structures: How Do Natural Gas Hydrates Form? *J. Chem. Phys.* **1999**, *110*, 11884−11889.
(7) Ramya, K. R.; Venkatnathan, A. Stability and Reactivity of Methane Clathrate Hydrates: Insights from Density Functional Theory. *J. Phys. Chem. A* **2012**, *116*, 7742−7745.
(8) Liu, Y.; Zhao, J.; Li, F.; Chen, Z. Appropriate Description of Intermolecular Interactions in the Methane Hydrates: An Assessment of DFT Methods. *J. Comput. Chem.* **2013**, *34*, 121−131.
(9) Dunning, T. H., Jr. Gaussian Basis Sets for Use in Correlated Molecular Calculations. I. The Atoms Boron Through Neon and Hydrogen. *J. Chem. Phys.* **1989**, *90*, 1007−1023.
(10) Bakowies, D. Accurate Extrapolation of Electron Correlation Energies from Small Basis Sets. *J. Chem. Phys.* **2007**, *127*, 164109-1−164109-12.
(11) Jiang, H.; Myshakin, E.; Jordan, K. D.; Warzinski, R. Molecular Dynamics Simulations of the Thermal Conductivity of Methane Hydrate. *J. Phys. Chem. B* **2008**, *112*, 10207−10216.
(12) Pitonak, M.; Hesselmann, A. Accurate Intermolecular Interaction Energies from a Combination of MP2 and TDDFT Response Theory. *J. Chem. Theory Comput.* **2010**, *6*, 168−178.
(13) Werner, H. J.; Adler, T. B.; Manby, F. R. General Orbital Invariant MP2-F12 Theory. *J. Chem. Phys.* **2007**, *126*, 164102-1−164102-18.
(14) Adler, T. B.; Knizia, G.; Werner, H.-J. A Simple and Efficient CCSD(T)-F12 Approximation. *J. Chem. Phys.* **2007**, *127*, 221106-1−221106-4.
(15) Werner, H.-J.; Knizia, G.; Manby, F. R. Explicitly Correlated Coupled Cluster Methods with Pair-Specific Geminals. *Mol. Phys.* **2011**, *109*, 407−417.
(16) Hesselmann, A.; Jansen, G.; Schutz, M. Density-Functional Theory-Symmetry-Adapted Intermolecular Perturbation Theory with Density Fitting: A New Efficient Method to Study Intermolecular Interaction Energies. *J. Chem. Phys.* **2005**, *122*, 014103-1−014103-17.
(17) Lotrich, V. F.; Szalewicz, K. Symmetry-Adapted Perturbation Theory of Three-Body Nonadditivity of Intermolecular Interaction Energy. *J. Chem. Phys.* **1997**, *106*, 9668−9687.
(18) Lotrich, V. F.; Szalewicz, K. Perturbation Theory of Three-Body Exchange Nonadditivity and Application to Helium Trimer. *J. Chem. Phys.* **2000**, *112*, 112−121.
(19) McDonald, S.; Ojamäe, L.; Singer, S. J. Graph Theoretical Generation and Analysis of Hydrogen-Bonded Structures with Applications to the Neutral and Protonated Water Cube and Dodecahedral Clusters. *J. Phys. Chem. A* **1998**, *102*, 2824−2832.
(20) Kirov, M. V.; Fanourgakis, G. S.; Xantheas, S. S. Identifying the Most Stable Networks in Polyhedral Water Clusters. *Chem. Phys. Lett.* **2008**, *461*, 180−188.
(21) Wales, D. J.; Hodges, M. P. Global Minima of Water Clusters $(H_2O)_n$, $n \leq 21$, Described by an Empirical Potential. *Chem. Phys. Lett.* **1998**, *286*, 65−72.
(22) Møller, C.; Plesset, M. S. Note on the Approximation Treatment for Many-Electron Systems. *Phys. Rev.* **1934**, *46*, 618−622.
(23) Werner, H.-J.; Manby, F. R.; Knowles, P. J. Fast Linear Scaling Second-Order Møller-Plesset Perturbation Theory (MP2) Using Local and Density Fitting Approximations. *J. Chem. Phys.* **2003**, *118*, 8149−8160.
(24) Zhao, Y.; Truhlar, D. G. The M06 Suite of Density Functionals for Main Group Thermochemistry, Thermochemical Kinetics, Noncovalent Interactions, Excited States, and Transition Elements: Two New Functionals and Systematic Testing of Four M06-class Functionals and 12 Other Functionals. *Theor. Chem. Acc.* **2008**, *120*, 215−241.
(25) Lee, C.; Yang, Wa.; Parr, R. G. Development of the Colle-Salvetti Correlation-Energy Formula into a Functional of the Electron Density. *Phys. Rev. B* **1988**, *37*, 785−789. Miehlich, B.; Savin, A.; Stoll, H.; Preuss, H. Results Obtained with the Correlation Energy Density Functionals of Becke and Lee, Yang and Parr. *Chem. Phys. Lett.* **1989**, *157*, 200−205. Becke, A. D. Density-functional Exchange-energy Approximation with Correct Asymptotic Behavior. *Phys. Rev. A* **1988**, *38*, 3098−3100.
(26) Perdew, J. P.; Burke, K.; Ernzerhof, M. Generalized Gradient Approximation Made Simple. *Phys. Rev. Lett.* **1996**, *77*, 3865−3868.
(27) Adamo, C.; Barone, V. Toward Reliable Density Functional Methods without Adjustable Parameters: The PBE0Model. *J. Chem. Phys.* **1999**, *110*, 6158−6170.
(28) Grimme, S.; Anthony, S.; Ehrlich, S.; Krieg, H. A Consistent and Accurate ab initio Parametrization of Density Functional Dispersion Correction (DFT-D) for the 94 Elements H-Pu. *J. Chem. Phys.* **2010**, *132*, 154104-1−154104-19.
(29) Schrader, D. M.; Prager, S. Use of Electrostatic Variation Principles in Molecular Energy Calculations. *J. Chem. Phys.* **1962**, *37*, 145614−60.
(30) Whitten, J. L. Coulombic Potential Energy Integrals and Approximations. *J. Chem. Phys.* **1973**, *58*, 4496−4501.
(31) Feller, D. The Use of Systematic Sequences of Wave Functions for Estimating the Complete Basis Set, Full Configuration Interaction Limit in Water. *J. Chem. Phys.* **1993**, *98*, 7059−7071.
(32) Helgaker, T.; Klopper, W.; Kock, H.; Noga, J. Basis-Set Convergence of Correlated Calculation of Water. *J. Chem. Phys.* **1997**, *106*, 9639−9646.
(33) Boys, S. F.; Bernardi, F. The Calculation of Small Molecular Interactions by the Differences of Separate Total Energies. Some Procedures with Reduced Errors. *Mol. Phys.* **1970**, *19*, 553−566.

(34) MOLPRO is a package of ab initio programs written by: Werner, H.-J.; Knowles, P. J.; Knizia, G.; Manby, F. R.; Schütz, M.; Celani, P.; Korona, T.; Lindh, R.; Mitrushenkov, A.; Rauhut, G.; et al.
(35) Becke, A. D. Density-Functional Thermochemistry. III. The Role of Exact Exchange. *J. Chem. Phys.* **1993**, *98*, 5648−5652. Lee, C.; Yang, W.; Parr, R. G. Development of the Colle-Salvetti Correlation-Energy Formula into a Functional of the Electron Density. *Phys. Rev. B* **1988**, *37*, 785−789.
(36) Trail, J. R.; Needs, R. J. Smooth Relativistic Hartree-Fock Pseudopotentials for H to Ba and Lu to Hg. *J. Chem. Phys.* **2005**, *122*, 174109-1−174109-10. Trail, J. R.; Needs, R. J. Norm-Conserving Hartree-Fock Pseudopotentials and Their Asymptotic Behavior. *J. Chem. Phys.* **2005**, *122*, 014112−01411211. See also: www.vallico.net/casinoqmc/pplib/.
(37) Xu, J.; Deible, M. J.; Peterson, K. A.; Jordan, K. D. Correlation Consistent Gaussian Basis Sets for H, B-Ne with Dirac-Fock AREP Pseudopotentials: Applications in Quantum Monte Carlo Calculations. *J. Chem. Theory Comput.* **2013**, *9*, 2170−2178.
(38) Drummond, N. D.; Towler, M. D.; Needs, R. J. Jastrow Correlation Factor for Atoms, Molecules, and Solids. *Phys. Rev. B* **2004**, *70*, 235119−235129.
(39) Casula, M. Beyond the Locality Approximation in the Standard Diffusion Monte Carlo Method. *Phys. Rev. B* **2006**, *74*, 161102-1−161102-4.
(40) Frisch, M. J.; Trucks, G. W.; Schlegel, H. B.; Scuseria, G. E.; Robb, M. A.; Cheeseman, J. R.; Scalmani, G.; Barone,V.; Mennucci, B.; Petersson, G. A.; et al. *Gaussian 09*, revision B.01; Gaussian, Inc.: Wallingford, CT, 2010.
(41) Needs, R. J.; Towler, M. D.; Drummond, N. D.; Rios, P. L. Continuum Variational and Diffesion Quantum Monre Carlo Calculations. *J. Phys.: Condens. Matter* **2010**, *22*, 023201-1−023201-15.
(42) Peterson, K. A.; Adler, T. B.; Werner, H.-J. Systematically Convergent Basis Sets for Explicitly Correlated Wavefunctions: The Atoms H, He, B-Ne, and Al-Ar. *J. Chem. Phys.* **2008**, *128*, 084102-1−084102-12.
(43) Zangwill, A.; Soven, P. Resonant Photoemission in Barium and Cerium. *Phys. Rev. Lett.* **1980**, *45*, 204−207.
(44) Koopmans, T. Über die Zuordnung von Wellenfunktionen und Eigenwerten zu den Einzelnen Elektronen Eines Atoms. *Physica* **1934**, *1*, 104−113.
(45) Cox, S. J.; Towler, M. D.; Alfè, D.; Michaelides, A. Preprint.
(46) Axilrod, B. M.; Teller, E. Interaction of the van der Waals Type between Three Atoms. *J. Chem. Phys.* **1943**, *11*, 299−300.
(47) Klimeš, J.; Bowler, D. R.; Michaelides, A. Chemical Accuracy for the van der Waals Density Functional. *J. Phys.: Condens. Matter* **2010**, *22*, 022201-1−022201-6.
(48) Gillan, M. J.; Manby, F. R.; Towler, M. D.; Alfe, D. Assessing the Accuracy of Quantum Monte Carlo and Density Functional Theory for Energetics of Small Water Clusters. *J. Chem. Phys.* **2012**, *136*, 244105-1−244105-14.
(49) Wang, F. F.; Jenness, G.; Al-Saidi, W. A.; Jordan, K. D. Assessment of the Performance of Common Density Functional Methods for Describing the Interaction Energies of $(H_2O)_6$ Clusters. *J. Chem. Phys.* **2010**, *132*, 134303-1−134303-8.